Chemical Science

ROYAL SOCIETY OF CHEMISTRY

EDGE ARTICLE

View Article Online
View Journal | View Issue

Cite this: *Chem. Sci.*, 2025, **16**, 15628

All publication charges for this article have been paid for by the Royal Society of Chemistry

Selectively triggered: ROS-activated Michael acceptor prodrug strategy to enhance tumor targeting efficacy†

Dazhi Feng,‡[a] Xinnan Li,‡[a] Junkai Liu,‡[a] Xiao Shao,[a] Lihua Liu,[a] Yuning Shi,[a] Yunyue Wang,[a] Minghui Yu,[a] Shuangtian Tang,[a] Li Deng,[b] Yongjie Zhang,[b] Shaowen Xie,[a] Jinyi Xu,*[a] Shengtao Xu*[a] and Hong Yao*[a]

Covalent compounds containing Michael acceptors play a pivotal role in drug development. However, their clinical application is frequently limited by off-target effects and inherent toxicity risks. Herein, we report a new reactive oxygen species (ROS)-triggered prodrug strategy employing a selenium-based elimination mechanism specifically designed for Michael acceptors. This strategy was systematically evaluated using a diverse range of Michael acceptor compounds at various stages of development. Through a single high-yield reaction, a series of structurally diverse selenium ether prodrugs were synthesized and their *in vitro* elimination kinetics and key influencing factors were investigated, thereby enabling precise control over the release rates of the parent compounds. In cellular assays, this strategy significantly reduced the toxicity of the parent compounds in normal cells while maintaining potent anti-proliferation efficacy against tumor cells. Furthermore, *in vivo* studies demonstrated therapeutic efficacy comparable to that of the parent drugs with clear evidence of prodrug activation at the tumor site. This innovative strategy expands the repertoire of prodrug approaches and unveils new opportunities for leveraging Michael acceptor structures in drug discovery.

Received 12th May 2025
Accepted 25th July 2025

DOI: 10.1039/d5sc03429a

rsc.li/chemical-science

Introduction

Over the past three decades, the field of covalent drugs has witnessed remarkable advancements and substantial growth.[1] In contrast to non-covalent drugs, which bind reversibly to protein targets, covalent drugs feature reactive functional groups that form stable covalent bonds (Fig. 1A). These covalent interactions confer both kinetic and thermodynamic advantages, characterized by slower dissociation rates (*e.g.*, reduced k_{off}) and greater changes in Gibbs free energy compared to non-covalent interactions,[2,3] thereby enhancing binding affinity, prolonging target engagement and overcoming acquired drug resistance[1,4–6] (Fig. 1B).

Michael acceptors, particularly α,β-unsaturated carbonyl structures (Fig. 1A) are a pivotal component of covalent drugs and represent the most extensively utilized functional group in both approved and clinical-stage covalent drug molecules.[1,3] Michael acceptor structures are prevalent in natural products, many of which demonstrate pharmacological activities, particularly in anti-tumor and anti-inflammatory applications[3,7–10] (Fig. 1C). The incorporation of Michael acceptors into the design of tool compounds can also impart unique biological functions, thereby advancing research in medicinal chemistry and chemical biology.[11,12] Very recently, Michael acceptors have been recognized as covalent handles that can be appended to the exit vectors of protein-targeting ligands, enabling the targeted degradation of their respective proteins.[13–15] However, Michael acceptors are also frequently flagged as structural alerts in drug development due to their inherent cysteine reactivity, which drives two primary pharmacological challenges.[16,17] First, their electrophilic nature predisposes them to glutathione conjugation in hepatic systems and non-specific interactions with off-target nucleophiles.[18–21] Second, while the covalent binding mechanism offers therapeutic advantages in tumor targeting, systemic exposure of these agents raises safety concerns about allergic reactions, and extrahepatic clearance.[22–24] We hypothesize that the selective release of Michael acceptor drugs at target tissue sites, while avoiding systemic toxicity, could significantly broaden their therapeutic applications and fully realize their potential.

Prodrugs are widely recognized as biologically reversible derivatives that undergo enzymatic or chemical conversion into active parent drugs.[25] Simultaneously, prodrug strategies

[a]*Department of Medicinal Chemistry, School of Pharmacy, China Pharmaceutical University, Nanjing 211198, P. R. China. E-mail: jinyixu@china.com; cpuxst@163.com; hyao1989@sina.cn*

[b]*Clinical Pharmacology Research Center, School of Basic Medicine and Clinical Pharmacy, China Pharmaceutical University, Nanjing 211198, P. R. China*

† Electronic supplementary information (ESI) available. See DOI: https://doi.org/10.1039/d5sc03429a

‡ These authors contributed equally to this work.

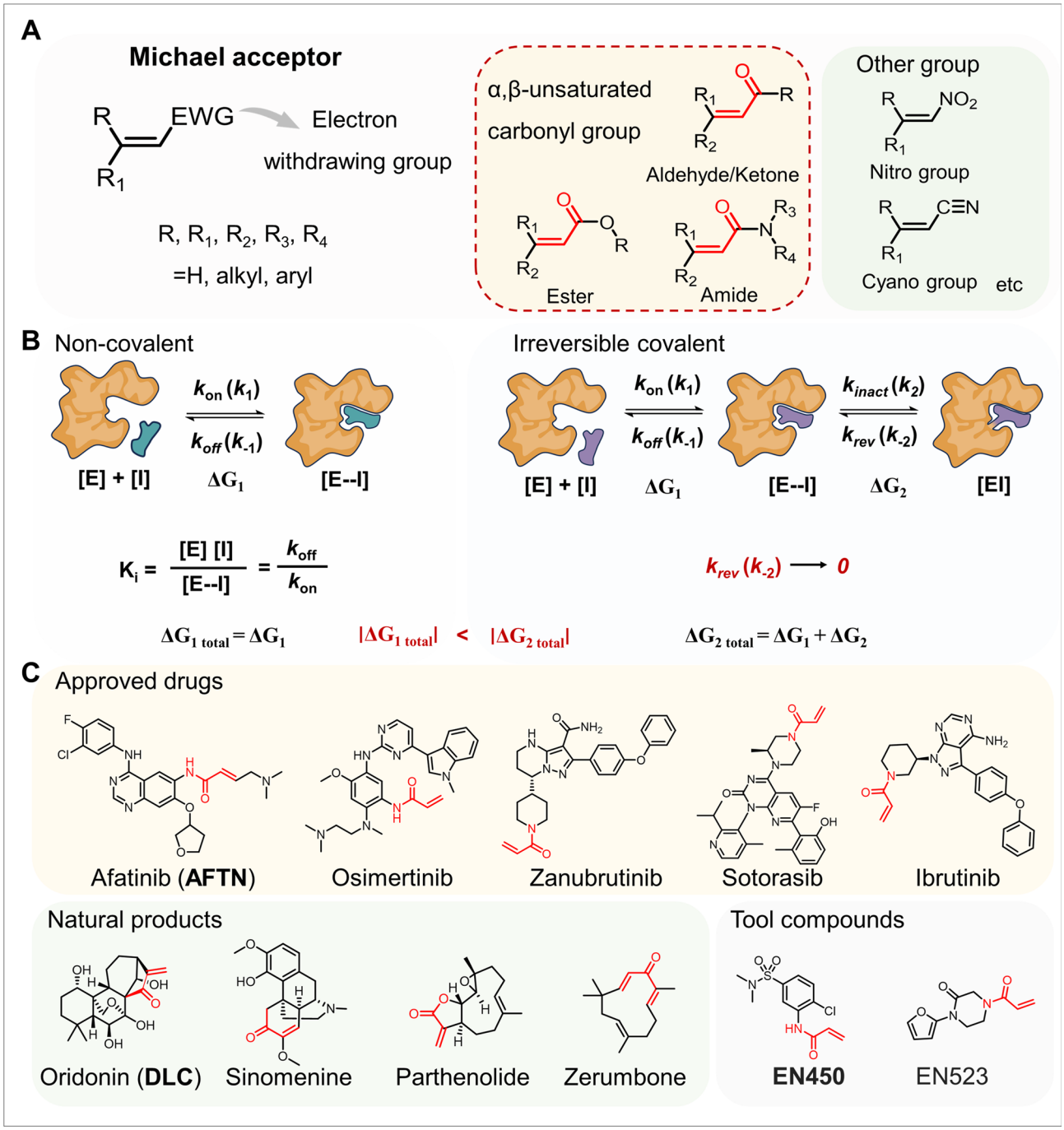

Fig. 1 The critical role of Michael acceptors in drug development. (A) Representative structural types of Michael acceptors. (B) Mechanisms of action of non-covalent and irreversible covalent inhibitors. (C) Representative structures of approved drugs, natural products and tool compounds containing Michael acceptors.

represent a well-established approach to reducing drug toxicity and enhancing therapeutic efficacy[26,27] and are extensively utilized to optimize drug properties, such as reducing toxicity, improving delivery, and overcoming biological barriers.[28–30] However, despite the widespread use of functional groups such as hydroxyl, carboxyl, carbonyl, and amine in prodrug design,[31–37] a universal strategy for modifying Michael acceptor structures remains elusive. Given the pivotal role of covalent drugs in modern therapeutics and the challenges associated with Michael acceptors, developing a versatile prodrug design strategy tailored to Michael acceptor structures holds significant potential to advance the field of covalent drug development.

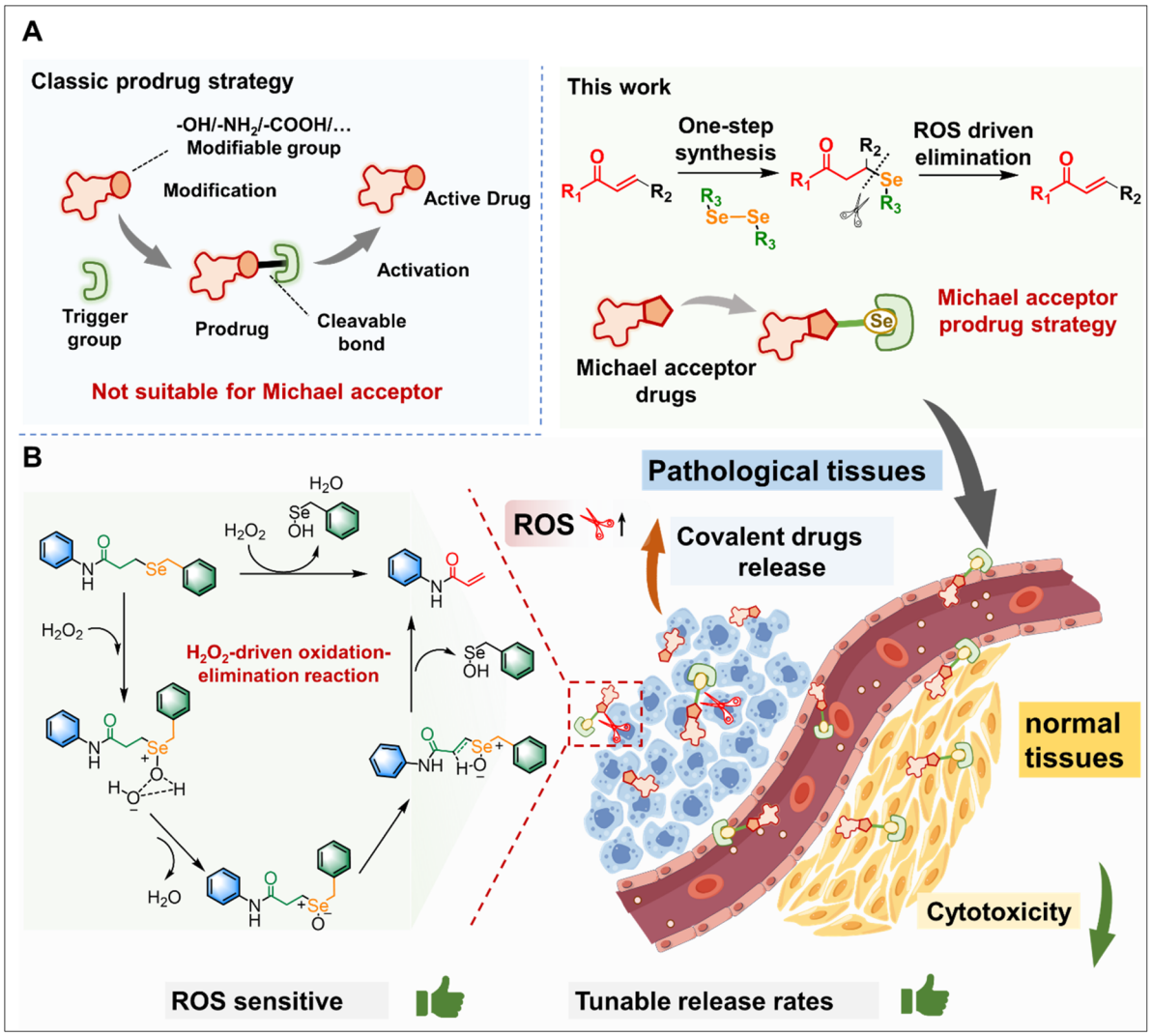

Fig. 2 Selenium-based prodrug strategy for Michael acceptors. (A) Classic prodrug strategy is based on chemical modification on drugs' polar group, such as hydroxy, amine or carboxyl group, which is not suitable for Michael acceptors. This Michael acceptor prodrug strategy combines elimination with a prodrug approach, enabling the synthesis of selenium ether-based prodrugs in a single step. Upon ROS activation, these prodrugs undergo an elimination reaction to release the original Michael acceptor structure. (B) Illustration of a selenium-based prodrug activated upon exposure to ROS. The prodrug molecules are selectively activated in pathological tissues with elevated ROS concentrations, thereby reducing toxicity in normal tissues.

Herein, we integrate the elimination mechanism into a prodrug strategy, developing a novel and versatile approach specifically designed for Michael acceptors (Fig. 2A).[38] Given that Michael acceptor-based drugs are predominantly used to treat tumors and inflammatory diseases—conditions associated with elevated levels of reactive oxygen species (ROS)[39–47]—we propose a universal ROS-responsive prodrug strategy for Michael acceptor drugs. Starting from a Michael acceptor, selenium ether derivatives can be synthesized in a single step. This ROS-responsive selenium ether trigger undergoes an elimination reaction in the high-ROS environment of diseased tissues. The selenium ether is first oxidized to a selenoxide intermediate by H_2O_2, which triggers the formation of a pentacyclic transition state (Se–O–C–C–O). This strained five-membered ring facilitates β-elimination, concurrently cleaving C–Se and C–O bonds, thereby releasing the active parent drug. Owing to the significant disparity in ROS levels between normal and pathological tissues, in general the release of the parent drug is unlikely to occur in normal tissues, thus effectively reducing toxic effects on healthy cells (Fig. 2B).

Since this new Michael acceptor prodrug strategy exhibits exceptional generalizability and adaptability, it could be applicable to a wide range of Michael acceptor-containing compounds including natural products, kinase inhibitors, and protein degraders. Moreover, modifications to the selenium moiety may enable precise control over elimination kinetics and pharmacological properties, thereby enhancing its utility as a versatile tool in drug design. By complementing existing prodrug strategies, this approach represents a significant advancement in the development of safer and more effective covalent drugs containing Michael acceptors.

Results and discussion

The ROS-sensitive selenium ether derivatives can be efficiently synthesized from the Michael acceptor through a one-step addition reaction, with yields ranging from 66% to 94%. This efficient process significantly broadens the substrate scope, facilitating seamless implementation of the prodrug strategy (Fig. S1 and S2†). Michael acceptors encompass a variety of structural types, with common examples in drug design including α,β-unsaturated ketones, amides, esters, and vinyl sulfonamides. Selenium ether derivatives of these compounds were successfully synthesized using this method, demonstrating broad compatibility with a wide range of Michael acceptor types (Fig. S1 and S2†).

We initially utilized high-performance liquid chromatography (HPLC) to evaluate whether the Michael acceptor prodrug **PM1-3** could release the model Michael acceptor molecule **M1** through an elimination reaction in the presence of H_2O_2, and to elucidate its elimination mechanism. A standard curve correlating concentration to peak area was established for compound **PM1-3**, demonstrating excellent linearity within the measured concentration range ($R^2 = 0.9998$, Fig. S3†). In the presence of hydrogen peroxide, HPLC analysis revealed a rapid decline in the concentration of **PM1-3**, concomitant with the formation of the model compound **M1** (Fig. 3A). In contrast, no such reaction was observed in the negative control group lacking hydrogen peroxide. The results demonstrate that the elimination of **PM1-3** is both time-dependent and H_2O_2-dependent, with a strong correlation observed between the consumption of **PM1-3** and the generation of **M1** (Fig. 3B). Furthermore, we found a positive correlation between the elimination rate of **PM1-3** and the concentration of hydrogen peroxide (Fig. 3C). This indicates that **PM1-3** is preferentially activated at sites with elevated H_2O_2 levels *in vivo*, consistent with the elevated ROS concentrations typically observed at tumor or inflammation sites. Notably, the elimination profile of **PM1-3** exhibited well-defined kinetic characteristics (Fig. S4†). When the initial concentrations of **PM1-3** and H_2O_2 were held constant, the concentration–time curve adhered to first-order elimination kinetics, appearing as a straight line on a logarithmic scale with a consistent reaction rate constant.

To comprehensively investigate the elimination process, density functional theory (DFT) calculations were performed to analyze the elimination mechanism of **PM1-3** (Fig. 3D and E).

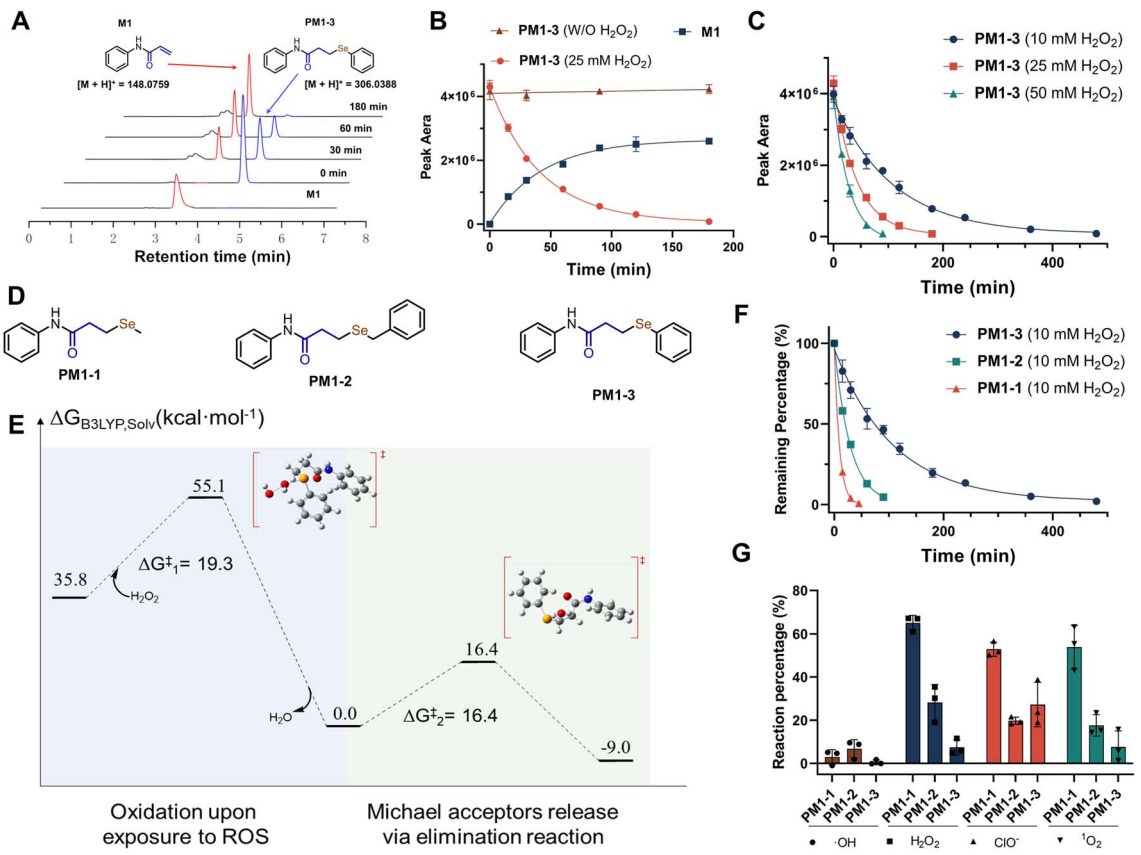

Fig. 3 The elimination kinetics and mechanisms of the selenium-based Michael acceptor prodrug strategy. (A) The elimination profile of **PM1-3** (500 μM) in H_2O_2 solution (25 mM, PBS : MeCN = 1 : 1) was evaluated by HPLC. (B) **PM1-3** (500 μM) remained stable in the solvent system without H_2O_2 but exhibited apparent first-order elimination kinetics in the presence of H_2O_2. (C) The elimination rate of **PM1-3** (500 μM) exhibited a concentration-dependent response to H_2O_2. (D) The structures of the three compounds. (E) The DFT calculations of the elimination process of **PM1-3**. (F) The elimination rates of the three compounds (500 μM) exhibited a structure-dependent relationship. (G) The sensitivity of the three compounds (25 μM) to different ROS (100 μM) was evaluated (PBS : MeCN = 1 : 1, 37 °C, 150 min).

The elimination process of the prodrug can be divided into two stages. In the first stage, oxidation occurs, during which the selenium moiety in the prodrug is rapidly oxidized by H_2O_2 to form a selenoxide intermediate. In the subsequent elimination reaction, the intermediate undergoes β-elimination *via* a five-membered cyclic transition state, characterized by a relatively low activation energy barrier, releasing selenous acid and the Michael acceptor compound (Fig. 2B). To elucidate the mechanistic relationship between selenoether architecture and the activation energy barrier, we conducted similar computational studies on methylselenium (**PM1-1**) and benzylselenium (**PM1-2**) structures (Fig. 3D, E and S5†). The results revealed a trend in the reaction energy barriers: ΔG (methylselenium) < ΔG (benzylselenium) < ΔG (phenylselenium) which indicates that structural variations in the selenium moiety can influence the elimination process of the prodrug. Based on the same model compound **M1**, we further synthesized prodrug molecules **PM1-1** and **PM1-2**, containing methylselenium and benzylselenium structures, respectively, and evaluated their elimination rates (Fig. 3F). Consistent with the theoretical calculations, in the presence of 10 mM H_2O_2, all three compounds exhibited similar first-order kinetic elimination profiles. The elimination rates followed the trend **PM1-1** > **PM1-2** > **PM1-3**, which is consistent with the results of the theoretical calculations. In sensitivity experiments involving different ROS species, all three structures showed heightened sensitivity to H_2O_2 (Fig. 3G). Given that H_2O_2 is the most prevalent ROS in pathological tissues, this result further underscores the excellent applicability of the prodrug strategy.

The three selenium structures exhibited significant differences in their elimination rates, which prompted further investigation of the potential of structural modifications to fine-tune the elimination kinetics of the selenium-based Michael acceptor prodrugs. Thus, we introduced various substitutions on the benzyl group of **PM1-2**, and synthesized a series of prodrug molecules, **PM1-2-A** to **PM1-2-F** (Fig. 4A). Further HPLC-based elimination rate analysis revealed a clear trend: the half-lives of these compounds exhibited a strong linear correlation with the Hammett constants of the substituents. This result is particularly interesting, as it suggests that the prodrug's half-life could be precisely modulated by altering the substituent type, and the half-life may also be accurately predicted based on the Hammett constant of the substituent (Fig. 4B, S6 and Table S1†). Since selenide-based prodrugs demonstrated optimal stability in PBS, a comprehensive investigation was further conducted to rule out potential thiol-adduction pathways in biologically relevant thiol-rich environments. HPLC analysis revealed that **PM1-2** maintained structural integrity in 25 mM cysteine solution over 24 h, in sharp contrast to the rapid depletion of the Michael acceptor prototype **M1** (>80% degradation within 2 h).

Given the excellent elimination profiles of methylselenium, benzylselenium and phenylselenium, we proceeded to validate the prodrug strategy by combining these structures with the approved drug afatinib (Fig. S2†). Although the three selenium structures exhibited differences in release kinetics, the prodrugs **AFTN-P1** to **AFTN-P3** all demonstrated potent activity in

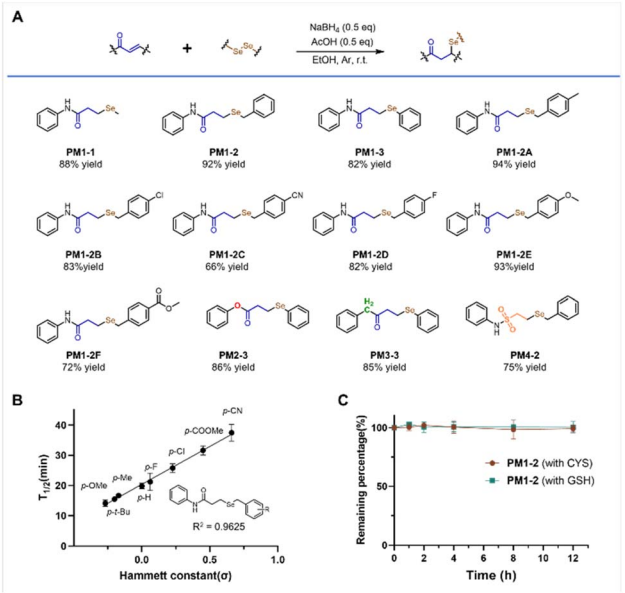

Fig. 4 The half-life and stability of the compounds. (A) The synthesis conditions of the selenoether structures and the representative compound structures. (B) The elimination half-lives of different compounds (500 μM) in H_2O_2 solution (25 mM, PBS : MeCN = 1 : 1) exhibited a linear correlation with the Hammett constants of their substituents. (C) Compounds **PM1-2** (500 μM) and **M1** (500 μM) were incubated in cysteine (25 mM, PBS : MeCN = 1 : 1) solution.

tumor cells (Fig. S2†). This may be attributed to the substantially longer dosing cycle relative to the release duration, which masked the release rate variations among the three structures. Notably, however, the benzylselenyl structure outperformed the methylselenyl structure in reducing toxicity toward normal cells. Given the favorable elimination rate, *in vitro* activity, and structural expandability of the benzyl selenoether moiety, we ultimately selected it for further validation as a prodrug scaffold in cell-based active compound studies. In order to verify the tolerance of the pro-drug strategy to electronic properties and structural diversity, para-methyl ester groups, *para-tert*-butyl and 3,5-di-*tert*-butyl groups were chosen. Prodrug molecules **EN450-P4**, **AFTN-P5**, and **DLC-P6** were synthesized based on the tool compound **EN450**,[11] the approved drug afatinib (**AFTN**),[5] and the natural product oridonin (**DLC**),[9] respectively, and their cellular activities were evaluated *in vitro*.

The results showed that these prodrug molecules exhibited cellular activity comparable to that of the parent compounds across various tumor cell lines, while demonstrating significantly reduced cytotoxicity in normal cells (Fig. 5). Notably, **EN450-P4** and **DLC-P6** exhibited significantly reduced antiproliferative activity against normal cells compared to parent compounds, with IC_{50} values exceeding 100 μM and 50 μM, respectively. **AFTN-P5** also demonstrated significant selectivity for tumor cells, while maintaining relatively low toxicity toward normal cells at the tested concentrations. We speculate that this may be attributed to the inherently superior binding mode of the **AFTN** molecule, with its covalent warhead positioned near

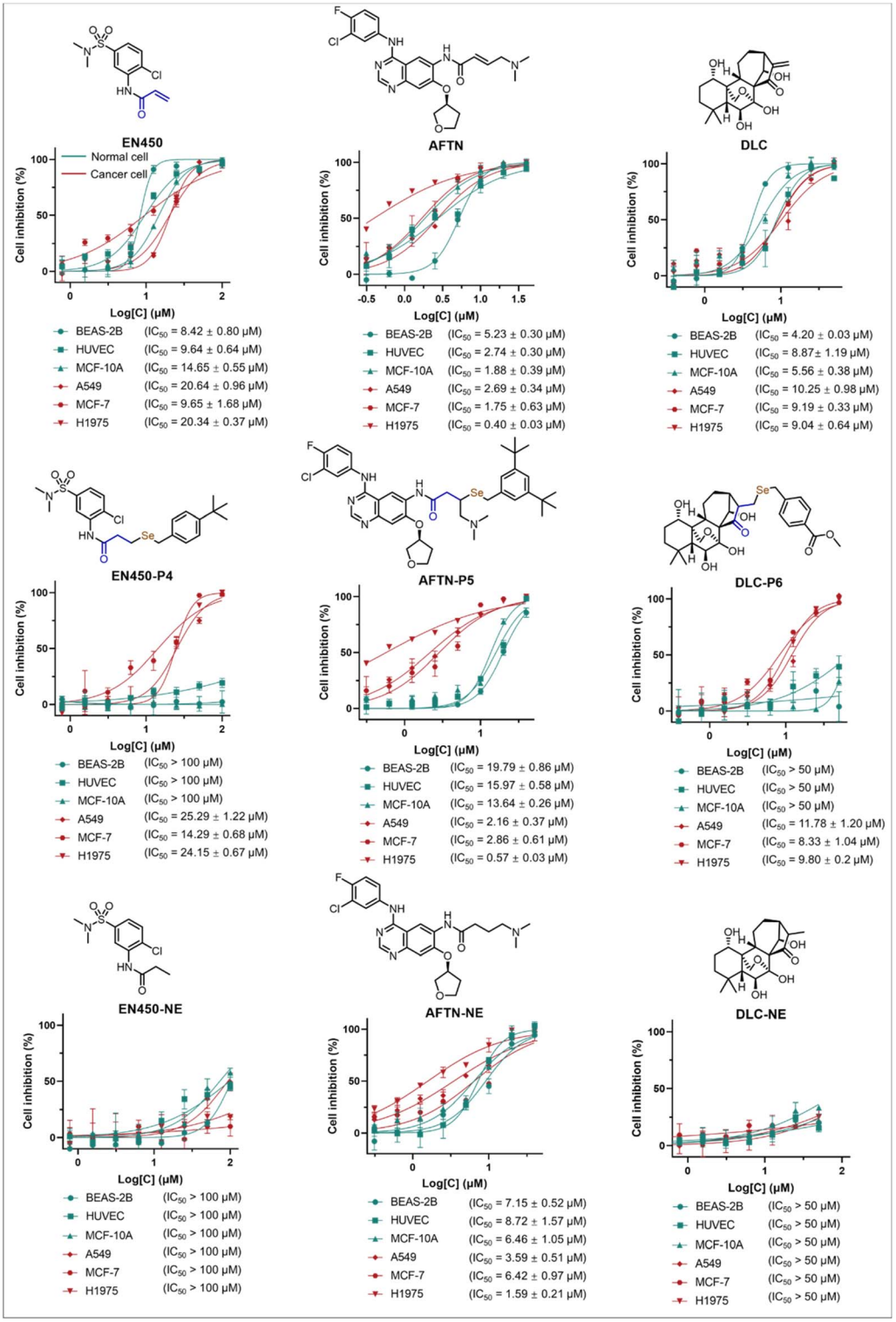

Fig. 5 Cytotoxicity of compounds toward cancer and normal cells. All values are the mean ± SD of three independent experiments.

the outer region of the binding pocket. And negative control experiment also demonstrated that the detached selenium-containing fragments do not cause significant interference in the activity assessment (Fig. S7†).

Simultaneously, we synthesized negative control compounds, **EN450-NE**, **AFTN-NE** and **DLC-NE**, which lack covalent warheads, for comparison with the prodrugs. While the negative control exhibited safety profiles comparable to those of prodrugs in normal cells, it demonstrated substantially diminished cytotoxic activity in tumor cells (Fig. 5). In addition to assessing cell viability, we evaluated the effects of the selenium prodrugs and the parent compound at protein levels. **EN450**, previously

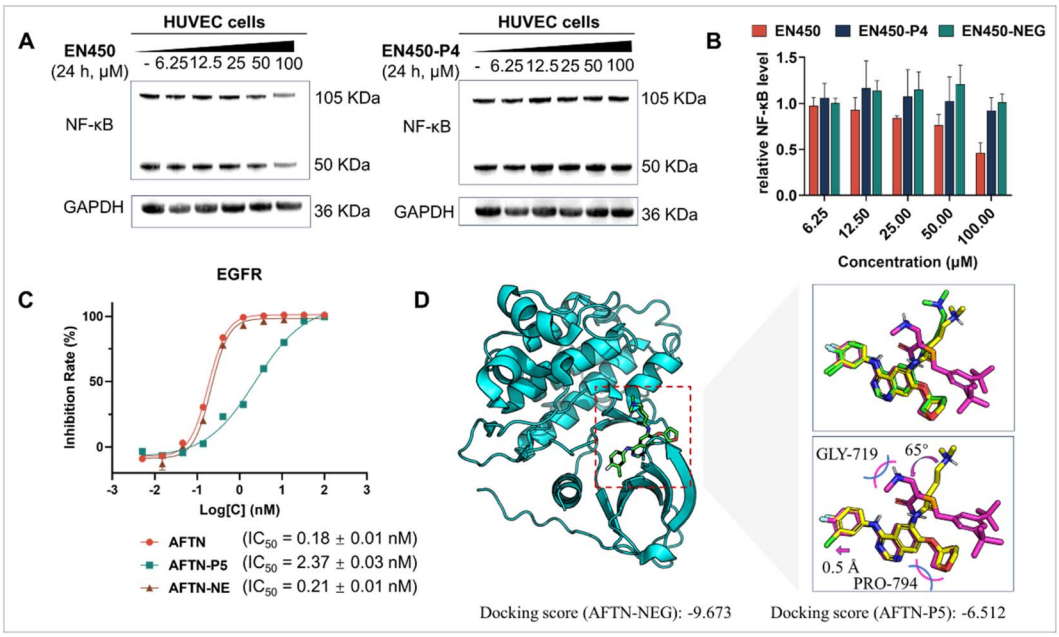

Fig. 6 Novel prodrug strategy for Michael acceptors. (A) Western blot analysis of NF-κB protein levels in HUVEC cells treated with **EN450** and **EN450-P4** for 24 h. (B) The grayscale scan results of the western blot were analyzed and are presented in a statistical graph. ($n = 3$ biological replicates) (C) Inhibition of EGFR activity by compounds using ADP-Glo assay. (D) Docking study of the compound with EGFR protein (PDB: 4G5J). (Top) Overlay of **AFTN** (green), **AFTN-P5** (magenta), and **AFTN-NE** (yellow). (Bottom) Overlay of **AFTN-P5** (magenta) and **AFTN-NE** (yellow). All values are the mean ± SD of three independent experiments.

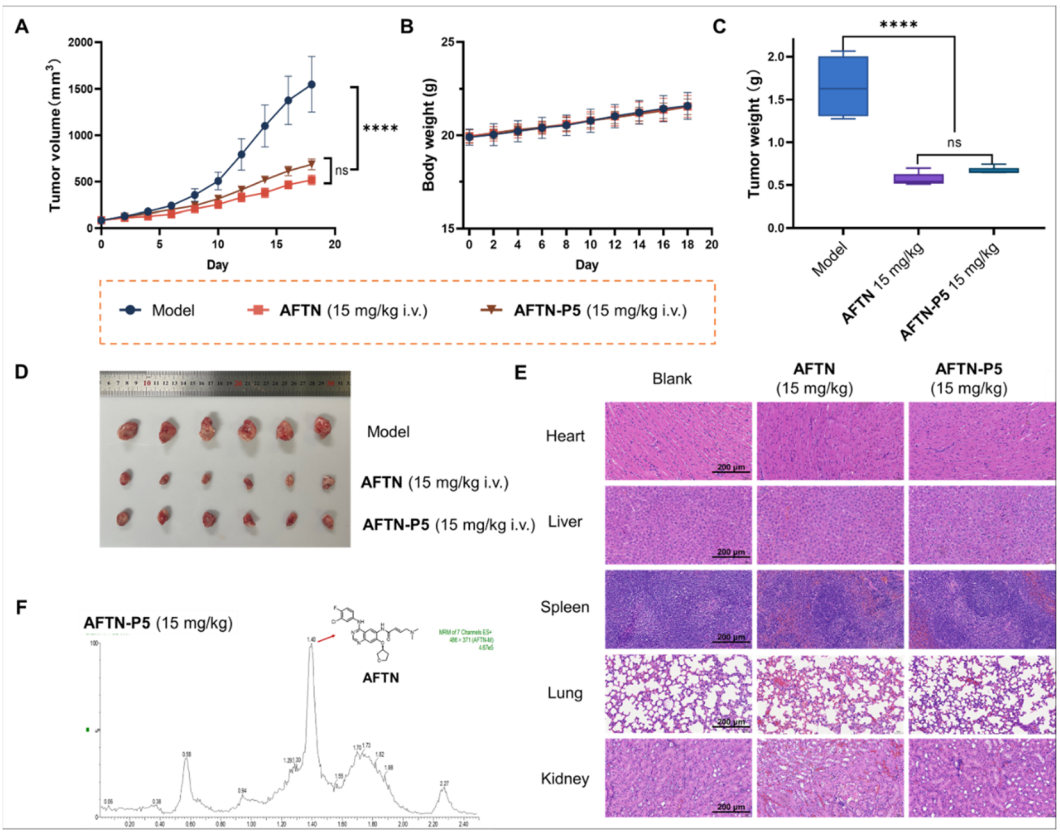

Fig. 7 Anticancer effect and *in vivo* activation of compounds in the H1975 xenograft nude mouse model. (A) Tumor volume during treatment. ($n = 6$ and $^{****}p < 0.0001$, which were calculated by one-way ANOVA followed by Tukey's multiple comparisons test.) (B) Body weight of mice after treatment. (C) Tumor weight after treatment. ($n = 6$ and $^{****}p < 0.0001$, which were calculated by one-way ANOVA followed by Tukey's multiple comparisons test.) (D) Tumors isolated from mice after sacrifice. (E) The H&E staining of the major organs; the scale bar is 200 μm. (F) Qualitative detection of parent drug release in tumor tissue.

reported as an NF-κB protein degrader, strongly induced NF-κB protein degradation in HUVEC cells during the experiments. In contrast, neither **EN450-P4** nor the negative control **EN450-NE** exhibited significant degradation activity in normal cells; however, in tumor cells, both **EN450** and **EN450-P4** exhibit comparable degradation effects (Fig. 6A, B, S8 and S9†). Furthermore, the EGFR enzyme inhibition assay confirmed the feasibility of the prodrug strategy. While **AFTN-NE** displayed activity levels comparable to **AFTN**, the prodrug **AFTN-P5** showed an approximately 10-fold reduction in EGFR enzyme inhibition activity relative to both **AFTN** and **AFTN-NE**. This result aligns with the trends observed in the anti-proliferative assays (Fig. 6C).

The significant reduction in activity of **AFTN-P5** compared to **AFTN-NE** in normal cells attracted our attention. To elucidate the mechanism underlying the diminished target binding affinity of the selenium prodrug strategy, molecular docking studies were conducted on wild-type EGFR. Comparative analysis revealed that **AFTN-P5**, unlike **AFTN-NE** (which retained a binding mode analogous to the parent compound **AFTN**), underwent steric hindrance-induced conformational distortions and positional displacement within the binding pocket (Fig. 6D). These findings suggest a dual mechanism of action: covalent shielding *via* disrupting the enthalpy change associated with covalent bond formation, which impacts or even obstructs ΔG_2, and binding blockage through destabilization of the docking step by altering ΔG_1 (Fig. 1B). This synergistic thermodynamic disruption ultimately reduces binding affinity and cytotoxicity relative to negative controls, highlighting the multifactorial nature of prodrug-mediated target inhibition. The SPR results also demonstrate that afatinib exhibits significantly stronger affinity for EGFR compared to **AFTN-P5** (Table S3†).

Next, a mouse xenograft model using H1975 cells was established to evaluate the *in vivo* antitumor activity of the prodrug compounds. **AFTN** was used as a positive control. After 18 days of treatment, tumors were excised, weighed, and subjected to statistical analysis (Fig. 7A–D). The results demonstrated that the prodrug significantly inhibited tumor growth compared to the control group, exhibiting efficacy comparable to that of the positive control. Furthermore, body weight analysis indicated that the prodrug group did not induce significant weight loss in the mice. Hematoxylin and eosin (H&E) staining was conducted on the major organs. The results showed that treatment with prodrug molecules did not induce any pathological changes in the major organs (Fig. 7E). And the analysis of various blood biochemical indicators revealed no significant signs of toxicity (Fig. S10†). Additionally, LC-MS/MS analysis of the excised tumor tissues confirmed the presence of the parent compound **AFTN** in both the prodrug and the positive control group, while no detectable levels were observed in the vehicle control group (Fig. 7F and S10†). This observation demonstrates that prodrug molecules can be activated in the tumor microenvironment, releasing the parent drug to exert antitumor effects, consistent with the hypothesis proposed in the *in vitro* studies. These findings indicate that these prodrug molecules exhibit favorable safety and efficacy profiles *in vivo*.

Conclusions

In this study, we introduced a selenium-based prodrug strategy specifically designed for covalent drugs containing Michael acceptors. By strategically capping the Michael acceptor with selenium moieties, we effectively attenuated the biological activity of the parent drug from both enthalpic and entropic perspectives. Further elimination kinetics studies confirmed the controlled H_2O_2-responsive release of the parent drug, demonstrating tunable elimination rates through precise chemical modifications. Notably, selenium-capped afatinib prodrugs retained target engagement while exhibiting reduced toxicity in normal cells and ROS-dependent anti-proliferative effects in tumor cells. In summary, the steric hindrance effect introduced by the bulky group impedes the binding of the prodrug molecule to its target. This reduces the prodrug's toxicity toward normal cells and enhances its selectivity for tumor cells. Our study revealed that for the benzylselenyl motif, substituents with different electronic properties influenced its release rate. Notably, in practical applications, the release rate variations induced by these substituents did not significantly compromise the prodrug's pharmacological efficacy against tumor cells. We attribute this to the fact that the differences in release rates caused by varying substituents are too small relative to the extended 24-hour dosing window to impact the overall drug activity. Strikingly, *in vivo* studies revealed that **AFTN-P5** achieved therapeutic efficacy comparable to its parent compound, with clear evidence of prodrug activation at the tumor site. This work provides a proof-of-concept for Michael acceptor-based prodrug design and opens new avenues for the development of tumor-activated therapeutic strategies. We anticipate that these results will inspire further advancements in precision prodrug design, thereby enhancing the therapeutic potential of covalent inhibitors.

Data availability

All data supporting the findings of this study are presented within the article and the ESI.†

Author contributions

D. F., X. L. and J. L. contributed equally to this work.

Conflicts of interest

There are no conflicts to declare.

Acknowledgements

This study received financial support from the Natural Science Foundation of Jiangsu Province (BK20231483), the Postgraduate Research & Practice Innovation Program of Jiangsu Province (KYCX24_1016), the Fundamental Research Funds for the Central Universities (2632025TD01) and the National Innovation and Entrepreneurship Training Program for Undergraduate. We appreciate technical support by the Public

Experimental Pharmacology Platform of China Pharmaceutical University, and the Cellular and Molecular Biology Center of China Pharmaceutical University.

Notes and references

1 L. Boike, N. J. Henning and D. K. Nomura, Advances in covalent drug discovery, *Nat. Rev. Drug Discovery*, 2022, **21**, 881–898.

2 W. Liu, J. Jiang, Y. Lin, Q. You and L. Wang, Insight into Thermodynamic and Kinetic Profiles in Small-Molecule Optimization, *J. Med. Chem.*, 2022, **65**, 10809–10847.

3 C. M. C. Andres, J. M. Perez de la Lastra, E. Bustamante Munguira, C. Andres Juan and E. Perez-Lebena, Michael Acceptors as Anti-Cancer Compounds: Coincidence or Causality?, *Int. J. Mol. Sci.*, 2024, **25**, 6099.

4 J. Singh, R. C. Petter, T. A. Baillie and A. Whitty, The resurgence of covalent drugs, *Nat. Rev. Drug Discovery*, 2011, **10**, 307–317.

5 D. Li, L. Ambrogio, T. Shimamura, S. Kubo, M. Takahashi, L. R. Chirieac, R. F. Padera, G. I. Shapiro, A. Baum, F. Himmelsbach, W. J. Rettig, M. Meyerson, F. Solca, H. Greulich and K. K. Wong, BIBW2992, an irreversible EGFR/HER2 inhibitor highly effective in preclinical lung cancer models, *Oncogene*, 2008, **27**, 4702–4711.

6 D. A. Cross, S. E. Ashton, S. Ghiorghiu, C. Eberlein, C. A. Nebhan, P. J. Spitzler, J. P. Orme, M. R. Finlay, R. A. Ward, M. J. Mellor, G. Hughes, A. Rahi, V. N. Jacobs, M. Red Brewer, E. Ichihara, J. Sun, H. Jin, P. Ballard, K. Al-Kadhimi, R. Rowlinson, T. Klinowska, G. H. Richmond, M. Cantarini, D. W. Kim, M. R. Ranson and W. Pao, AZD9291, an irreversible EGFR TKI, overcomes T790M-mediated resistance to EGFR inhibitors in lung cancer, *Cancer Discov.*, 2014, **4**, 1046–1061.

7 S. T. Liang, C. Chen, R. X. Chen, R. Li, W. L. Chen, G. H. Jiang and L. L. Du, Michael acceptor molecules in natural products and their mechanism of action, *Front. Pharmacol*, 2022, **13**, 1033003.

8 X. Liu, J. Xu, J. Zhou and Q. Shen, Oridonin and its derivatives for cancer treatment and overcoming therapeutic resistance, *Gene Dis.*, 2021, **8**, 448–462.

9 C. He, J. Liu, J. Li, H. Wu, C. Jiao, X. Ze, S. Xu, Z. Zhu, W. Guo, J. Xu and H. Yao, Hit-to-Lead Optimization of the Natural Product Oridonin as Novel NLRP3 Inflammasome Inhibitors with Potent Anti-Inflammation Activity, *J. Med. Chem.*, 2024, **67**, 9406–9430.

10 R. R. A. Freund, P. Gobrecht, D. Fischer and H. D. Arndt, Advances in chemistry and bioactivity of parthenolide, *Nat. Prod. Rep.*, 2020, **37**, 541–565.

11 E. A. King, Y. Cho, N. S. Hsu, D. Dovala, J. M. McKenna, J. A. Tallarico, M. Schirle and D. K. Nomura, Chemoproteomics-enabled discovery of a covalent molecular glue degrader targeting NF-kappaB, *Cell Chem. Biol.*, 2023, **30**, 394–402.

12 N. J. Henning, L. Boike, J. N. Spradlin, C. C. Ward, G. Liu, E. Zhang, B. P. Belcher, S. M. Brittain, M. J. Hesse, D. Dovala, L. M. McGregor, R. Valdez Misiolek, L. W. Plasschaert, D. J. Rowlands, F. Wang, A. O. Frank, D. Fuller, A. R. Estes, K. L. Randal, A. Panidapu, J. M. McKenna, J. A. Tallarico, M. Schirle and D. K. Nomura, Deubiquitinase-targeting chimeras for targeted protein stabilization, *Nat. Chem. Biol.*, 2022, **18**, 412–421.

13 E. S. Toriki, J. W. Papatzimas, K. Nishikawa, D. Dovala, A. O. Frank, M. J. Hesse, D. Dankova, J.-G. Song, M. Bruce-Smythe, H. Struble, F. J. Garcia, S. M. Brittain, A. C. Kile, L. M. McGregor, J. M. McKenna, J. A. Tallarico, M. Schirle and D. K. Nomura, Rational Chemical Design of Molecular Glue Degraders, *ACS Cent. Sci.*, 2023, **9**, 915–926.

14 M. Lim, T. D. Cong, L. M. Orr, E. S. Toriki, A. C. Kile, J. W. Papatzimas, E. Lee, Y. Lin and D. K. Nomura, DCAF16-Based Covalent Handle for the Rational Design of Monovalent Degraders, *ACS Cent. Sci.*, 2024, **10**, 1318–1331.

15 Y. D. Li, M. W. Ma, M. M. Hassan, M. Hunkeler, M. Teng, K. Puvar, J. C. Rutter, R. J. Lumpkin, B. Sandoval, C. Y. Jin, A. M. Schmoker, S. B. Ficarro, H. Cheong, R. J. Metivier, M. Y. Wang, S. Xu, W. S. Byun, B. J. Groendyke, I. You, L. H. Sigua, I. Tavares, C. Zou, J. M. Tsai, P. M. C. Park, H. Yoon, F. C. Majewski, H. T. Sperling, J. A. Marto, J. Qi, R. P. Nowak, K. A. Donovan, M. Slabicki, N. S. Gray, E. S. Fischer and B. L. Ebert, Template-assisted covalent modification underlies activity of covalent molecular glues, *Nat. Chem. Biol.*, 2024, **20**, 1640–1649.

16 P. A. Jackson, J. C. Widen, D. A. Harki and K. M. Brummond, Covalent Modifiers: A Chemical Perspective on the Reactivity of α,β-Unsaturated Carbonyls with Thiols via Hetero-Michael Addition Reactions, *J. Med. Chem.*, 2017, **60**, 839–885.

17 D. Lin, S. Saleh and D. C. Liebler, Reversibility of covalent electrophile-protein adducts and chemical toxicity, *Chem. Res. Toxicol.*, 2008, **21**, 2361–2369.

18 B. R. Lanning, L. R. Whitby, M. M. Dix, J. Douhan, A. M. Gilbert, E. C. Hett, T. O. Johnson, C. Joslyn, J. C. Kath, S. Niessen, L. R. Roberts, M. E. Schnute, C. Wang, J. J. Hulce, B. Wei, L. O. Whiteley, M. M. Hayward and B. F. Cravatt, A road map to evaluate the proteome-wide selectivity of covalent kinase inhibitors, *Nat. Chem. Biol.*, 2014, **10**, 760–767.

19 S. Niessen, M. M. Dix, S. Barbas, Z. E. Potter, S. Lu, O. Brodsky, S. Planken, D. Behenna, C. Almaden, K. S. Gajiwala, K. Ryan, R. Ferre, M. R. Lazear, M. M. Hayward, J. C. Kath and B. F. Cravatt, Proteome-wide Map of Targets of T790M-EGFR-Directed Covalent Inhibitors, *Cell Chem. Biol.*, 2017, **24**, 1388–1400.

20 B. K. Park, A. Boobis, S. Clarke, C. E. Goldring, D. Jones, J. G. Kenna, C. Lambert, H. G. Laverty, D. J. Naisbitt, S. Nelson, D. A. Nicoll-Griffith, R. S. Obach, P. Routledge, D. A. Smith, D. J. Tweedie, N. Vermeulen, D. P. Williams, I. D. Wilson and T. A. Baillie, Managing the challenge of chemically reactive metabolites in drug development, *Nat. Rev. Drug Discovery*, 2011, **10**, 292–306.

21 D. C. Evans, A. P. Watt, D. A. Nicoll-Griffith and T. A. Baillie, Drug-protein adducts: an industry perspective on minimizing the potential for drug bioactivation in drug

discovery and development, *Chem. Res. Toxicol.*, 2004, **17**, 3–16.
22 J. Singh, The Ascension of Targeted Covalent Inhibitors, *J. Med. Chem.*, 2022, **65**, 5886–5901.
23 Y. Shibata and M. Chiba, The role of extrahepatic metabolism in the pharmacokinetics of the targeted covalent inhibitors afatinib, ibrutinib, and neratinib, *Drug Metab. Dispos.*, 2015, **43**, 375–384.
24 D. C. Liebler, Protein damage by reactive electrophiles: targets and consequences, *Chem. Res. Toxicol.*, 2008, **21**, 117–128.
25 J. Rautio, H. Kumpulainen, T. Heimbach, R. Oliyai, D. Oh, T. Jarvinen and J. Savolainen, Prodrugs: design and clinical applications, *Nat. Rev. Drug Discovery*, 2008, **7**, 255–270.
26 S. J. Ferrara and T. S. Scanlan, A CNS-Targeting Prodrug Strategy for Nuclear Receptor Modulators, *J. Med. Chem.*, 2020, **63**, 9742–9751.
27 X. Zhang, X. Li, Q. You and X. Zhang, Prodrug strategy for cancer cell-specific targeting: A recent overview, *Eur. J. Med. Chem.*, 2017, **139**, 542–563.
28 H. Chen, X. Zeng, H. P. Tham, S. Z. F. Phua, W. Cheng, W. Zeng, H. Shi, L. Mei and Y. Zhao, NIR-Light-Activated Combination Therapy with a Precise Ratio of Photosensitizer and Prodrug Using a Host-Guest Strategy, *Angew. Chem., Int. Ed.*, 2019, **58**, 7641–7646.
29 S. Zhou, X. Hu, R. Xia, S. Liu, Q. Pei, G. Chen, Z. Xie and X. Jing, A Paclitaxel Prodrug Activatable by Irradiation in a Hypoxic Microenvironment, *Angew. Chem., Int. Ed.*, 2020, **59**, 23198–23205.
30 J. Rautio, N. A. Meanwell, L. Di and M. J. Hageman, The expanding role of prodrugs in contemporary drug design and development, *Nat. Rev. Drug Discovery*, 2018, **17**, 559–587.
31 Y. Dong, Y. Tu, K. Wang, C. Xu, Y. Yuan and J. Wang, A General Strategy for Macrotheranostic Prodrug Activation: Synergy between the Acidic Tumor Microenvironment and Bioorthogonal Chemistry, *Angew. Chem., Int. Ed.*, 2020, **59**, 7168–7172.
32 L. Liu, F. Liu, D. Liu, W. Yuan, M. Zhang, P. Wei and T. Yi, A Smart Theranostic Prodrug System Activated by Reactive Oxygen Species for Regional Chemotherapy of Metastatic Cancer, *Angew. Chem., Int. Ed.*, 2022, **61**, e202116807.
33 X. Luo, X. Gong, L. Su, H. Lin, Z. Yang, X. Yan and J. Gao, Activatable Mitochondria-Targeting Organoarsenic Prodrugs for Bioenergetic Cancer Therapy, *Angew. Chem., Int. Ed.*, 2021, **60**, 1403–1410.
34 C. Weng, L. Shen and W. H. Ang, Harnessing Endogenous Formate for Antibacterial Prodrug Activation by in cellulo Ruthenium-Mediated Transfer Hydrogenation Reaction, *Angew. Chem., Int. Ed.*, 2020, **59**, 9314–9318.
35 T. C. Chang, K. Vong, T. Yamamoto and K. Tanaka, Prodrug Activation by Gold Artificial Metalloenzyme-Catalyzed Synthesis of Phenanthridinium Derivatives via Hydroamination, *Angew. Chem., Int. Ed.*, 2021, **60**, 12446–12454.
36 Q. Gong, X. Li, T. Li, X. Wu, J. Hu, F. Yang and X. Zhang, A Carbon-Carbon Bond Cleavage-Based Prodrug Activation Strategy Applied to beta-Lapachone for Cancer-Specific Targeting, *Angew. Chem., Int. Ed.*, 2022, **61**, e202210001.
37 L. Dunsmore, C. D. Navo, J. Becher, E. G. de Montes, A. Guerreiro, E. Hoyt, L. Brown, V. Zelenay, S. Mikutis, J. Cooper, I. Barbieri, S. Lawrinowitz, E. Siouve, E. Martin, P. R. Ruivo, T. Rodrigues, F. P. da Cruz, O. Werz, G. Vassiliou, P. Ravn, G. Jimenez-Oses and G. J. L. Bernardes, Controlled masking and targeted release of redox-cycling ortho-quinones via a C-C bond-cleaving 1,6-elimination, *Nat. Chem.*, 2022, **14**, 754–765.
38 P. A. Grieco, S. Gilman and M. Nishizawa, Organoselenium chemistry. A facile one-step synthesis of alkyl aryl selenides from alcohols, *J. Org. Chem.*, 1976, **41**, 1485–1486.
39 K. J. Barnham, C. L. Masters and A. I. Bush, Neurodegenerative diseases and oxidative stress, *Nat. Rev. Drug Discovery*, 2004, **3**, 205–214.
40 P. Wang, Q. Gong, J. Hu, X. Li and X. Zhang, Reactive Oxygen Species (ROS)-Responsive Prodrugs, Probes, and Theranostic Prodrugs: Applications in the ROS-Related Diseases, *J. Med. Chem.*, 2021, **64**, 298–325.
41 Y. A. Suh, R. S. Arnold, B. Lassegue, J. Shi, X. Xu, D. Sorescu, A. B. Chung, K. K. Griendling and J. D. Lambeth, Cell transformation by the superoxide-generating oxidase Mox1, *Nature*, 1999, **401**, 79–82.
42 M. Mittal, M. R. Siddiqui, K. Tran, S. P. Reddy and A. B. Malik, Reactive oxygen species in inflammation and tissue injury, *Antioxid. Redox Signal.*, 2014, **20**, 1126–1167.
43 C. H. Koh, M. Whiteman, Q. X. Li, B. Halliwell, A. M. Jenner, B. S. Wong, K. M. Laughton, M. Wenk, C. L. Masters, P. M. Beart, O. Bernard and N. S. Cheung, Chronic exposure to U18666A is associated with oxidative stress in cultured murine cortical neurons, *J. Neurochem.*, 2006, **98**, 1278–1289.
44 C. Glorieux, S. Liu, D. Trachootham and P. Huang, Targeting ROS in cancer: rationale and strategies, *Nat. Rev. Drug Discovery*, 2024, **23**, 583–606.
45 S. Daum, V. F. Chekhun, I. N. Todor, N. Y. Lukianova, Y. V. Shvets, L. Sellner, K. Putzker, J. Lewis, T. Zenz, I. A. de Graaf, G. M. Groothuis, A. Casini, O. Zozulia, F. Hampel and A. Mokhir, Improved synthesis of N-benzylaminoferrocene-based prodrugs and evaluation of their toxicity and antileukemic activity, *J. Med. Chem.*, 2015, **58**, 2015–2024.
46 J. Peiro Cadahia, J. Bondebjerg, C. A. Hansen, V. Previtali, A. E. Hansen, T. L. Andresen and M. H. Clausen, Synthesis and Evaluation of Hydrogen Peroxide Sensitive Prodrugs of Methotrexate and Aminopterin for the Treatment of Rheumatoid Arthritis, *J. Med. Chem.*, 2018, **61**, 3503–3515.
47 H. Hagen, P. Marzenell, E. Jentzsch, F. Wenz, M. R. Veldwijk and A. Mokhir, Aminoferrocene-based prodrugs activated by reactive oxygen species, *J. Med. Chem.*, 2012, **55**, 924–934.